proceedings

MDPI

Proceedings

Characterization Procedure for Bond, Anchorage and Strain-Hardening Behavior of Textile-Reinforced Cementitious Composites †

Jan Bielak *, Yingxiong Li, Josef Hegger and Rostislav Chudoba

Institute of Structural Concrete, RWTH Aachen University, 52074 Aachen, Germany;
liyingxiong@live.com (Y.L.); jhegger@imb.rwth-aachen.de (J.H.); rchudoba@imb.rwth-aachen.de (R.C.)
* Correspondence: jbielak@imb.rwth-aachen.de; Tel.: +49-241-80-26830
† Presented at the 18th International Conference on Experimental Mechanics, Brussels, Belgium, 1–5 July 2018.

Published: 15 May 2018

Abstract: A fast adoption of innovative composite materials such as textile reinforced concrete (TRC) in practice is hindered by the lack of efficient and standardized characterization and design procedures. In this paper, we discuss results of uniaxial tensile tests and double sided pullout tests. The analysis of the tests is done with a modelling framework for tensile behavior developed at IMB RWTH Aachen. The overall goal is to simulate the tensile response of composite specimen based on the reinforcement and matrix characteristics. Thus, the need for cost-intensive composite tensile tests could be reduced, which facilitates the material development and adoption of TRC in engineering practice.

Keywords: pullout test; tensile test; anchorage length; strain-hardening behavior

1. Introduction

Development of innovative composite materials combining high-strength reinforcement with fine-grained matrices aims to achieve higher levels of efficiency and durability of future infrastructure than possible today. Still, despite remarkable progress of research achieved in last two decades, a wider application of textile-reinforced concrete structures is hindered by the lack of standardized, efficient characterization and design procedures [1]. To date, for many projects utilizing TRC, cost-intensive uniaxial tensile tests of the composite material are necessary in order to determine the stress strain behavior, the crack width and crack distribution. Especially for reinforcement with low bond stress, the required specimens are overly long and difficult to handle. Alternatively, the reinforcement needs special treatment prior to concreting, which may influence the experimental results. In this paper, we propose an approach for identification of the basic material characteristics and a subsequent simulation of the stress strain behavior. Eventually, such simulations could replace project specific uniaxial tensile tests on the composite.

2. Materials and Methods

2.1. Cementitious Matrix

The matrix used in this study is a fine-grained readymade mixture which was designed for repair and strengthening with textile reinforced concrete [2]. The bending tensile strength and the compressive strength were determined according to DIN EN 196-1 at the day of testing of the uniaxial tensile specimens. The mean values of the three batches are shown in Table 1. The modulus of

elasticity was determined on four cylindrical specimen (d/h = 100/200 mm) in accordance with DIN EN 12390-13 to 32,700 MPa with a coefficient of variation (CoV) of 4.1%.

Table 1. Concrete strength determined according to DIN EN 196-1.

Batch No. (Age)	Bending Tensile Strength [MPa]	CoV [%]	Compressive Strength [MPa]	CoV [%]
1 (27 d)	4.66	3.9	88.55	3.3
2 (27 d)	5.03	6.9	93.80	4.0
3 (28 d)	4.63	2.6	96.80	5.2

2.2. Reinforcement

As reinforcement, an impregnated biaxial carbon grid similar to [2] has been used. The impregnation material, styrene-butadiene-rubber, has been applied as aqueous dispersion and cured by the manufacturer. In the experiments, the test direction was aligned to the production direction (0°) of the textile. Each warp yarn has a cross-sectional area of 1.84 mm² with a spacing of 12.8 mm, the weft yarns with 0.45 mm² spaced at a distance of 16 mm center-to-center. The ultimate tensile strength and modulus of elasticity were determined in 20 single-yarn tensile tests at Technical University Dresden to 2739.7 MPa (COV 6.8%) and 256100 MPa (COV 3.4 %), respectively.

2.3. Tensile Tests

The tensile test setup used for the characterization of tensile response of the composite material follows the recommendations described in [3,4]. Here, the test force was applied by load-control with a velocity of 7.1 kN/min, which corresponds to a speed of 1 mm/min in saturated cracked stage IIb. Figure 1 shows two versions of the setup used in this study. For the short specimens (120 cm), the textile was coated with epoxy-resin and sprinkled with quartz sand in the anchorage zone prior to casting of the concrete. The fabrics used for the long specimens were not modified. A sufficient anchorage in setup (b) has been provided by the longer projecting length, which starts after the clamping zone. In total, 6 short and 6 long specimens were tested. The cross-section of both types was planned as w/t = 100/15 mm, with one centric layer of textile containing 8 warp yarns.

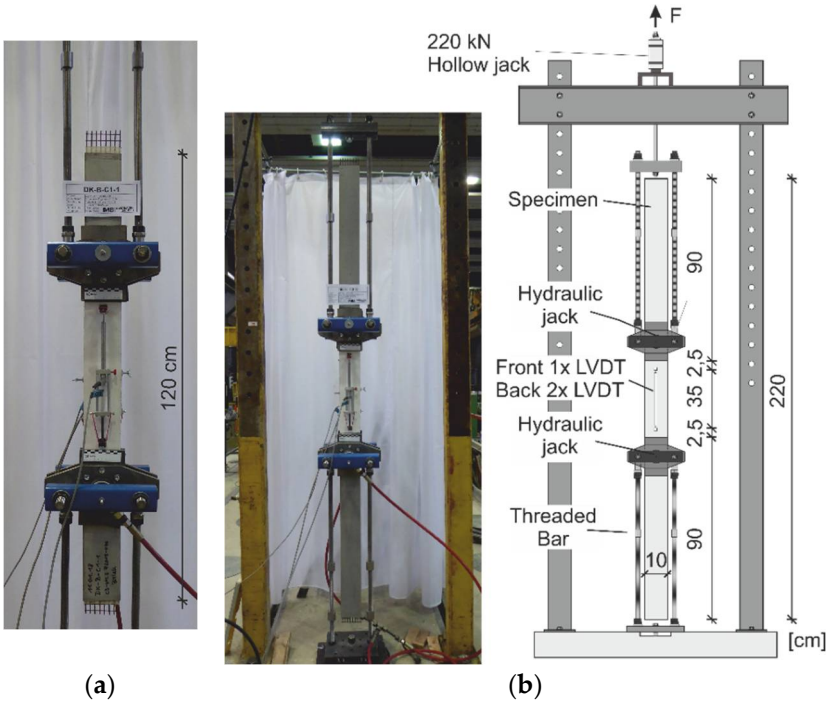

(**a**) (**b**)

Figure 1. (**a**) Tensile test setup for specimen with additional coating with epoxy-resin and quartz sand in the anchorage zone; (**b**) Long tensile test setup for realistic anchorage conditions.

2.4. Double-Sided-Pullout Tests

In order to determine the bond and anchorage behavior of the reinforcement, double-sided pullout tests were conducted. From each long specimen that was tested in uniaxial tension, at both ends the last, undamaged part of 20 cm was cut off and prepared with a horizontal notch of about 3 mm on both faces. Thus, a total of 12 specimens with an embedment length of 10 cm on each side could be obtained. The test setup and the testing procedure is described in [5]. The test velocity was 1 mm/min, and the test was displacement-controlled.

2.5. Incremental Inverse Analysis Procedure

In order to derive local bond-slip laws which serve as input for the numerical simulation, an incremental inverse analysis procedure developed at IMB RWTH has been used. The finite-element based procedure is explained in detail in [6]. It increases a control parameter stepwise—here, the slip on the loaded end was chosen—and solves the pull-out problem for each displacement step. As the maximum slip always occurs on the loaded end, one can conclude that every value for the local bond stress along the embedded length must have occurred once (and first) at the loaded end, which is for the double-sided pullout test the position of the notch. By solving the boundary value problem for each step and calculating the current pullout force, each point of the bond-slip law can be calibrated in such a way that the equilibrium of forces is satisfied. The result of this analysis is obtained in form of are a multilinear bond-slip functions without any restrictions on their shape.

2.6. Simulation of Stress-Strain Behavior of Cracked Composite Specimen

With known material characteristics of both matrix and reinforcement as well as the bond properties, the simulation of the stress-strain response and the cracking process is possible. The model used for this study was introduced in [7]. For the simulation, a defined length of a specimen is decomposed into a series of crack bridges. By pre-solving the crack bridge model for multiple lengths and pull-out forces, a response surface is constructed describing the behavior of a crack bridge within the tensile test specimen. The crack tracing algorithm utilizes this response surface to determine the crack locations, crack width and matrix stress levels along the specimen during the loading process. In this study, a random matrix strength along the specimen length was assumed.

3. Results

3.1. Uniaxial Tensile Tests

Both types of tensile specimen could be tested successfully with the chosen setup. For one long specimen, only the maximum force was recorded due to a malfunction of instrumentation. Figure 2 allows for a comparison of the stress-strain responses for both types. At first glance, the scatter of the short specimen seems higher. Regarding only the maximum tensile stress and the elastic modulus in saturated cracked state (IIb, after formation of the last crack), the magnitude of scatter is comparable (Table 2). Note that the relatively low number of cracks in the measuring range highly influences both the ultimate strain and the stiffness in state IIb. As the effective bond stress for this textile is relatively low, a long transfer length and a large crack spacing can be observed.

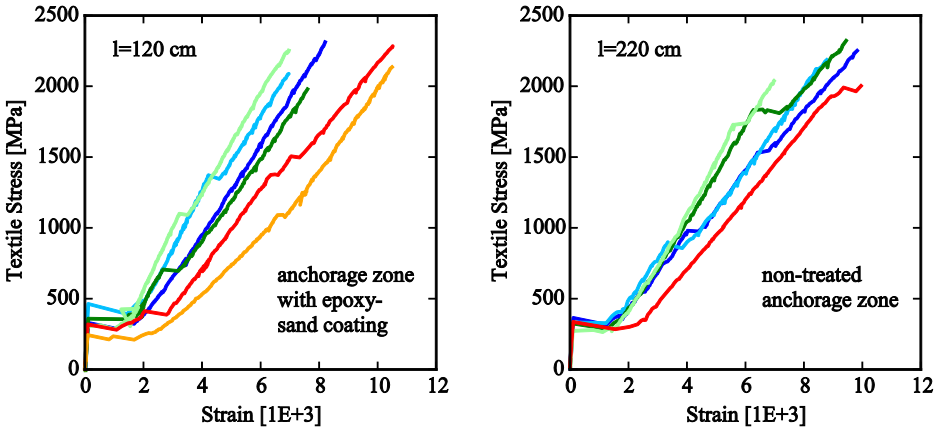

Figure 2. Stress-strain diagrams for specimen with (**a**) add. coating, (**b**) non-treated anchorage zone.

Table 2. Results of tensile tests.

Anchorage w. Additional Coating (120 cm)				Non-Treated Anchorage (220 cm)			
	$\sigma_{t,u}$	E (IIb)	No. Cracks [1]		$\sigma_{t,u}$	E (IIb)	No. Cracks [1]
No.	[MPa]	[MPa]	[-]	No.	[MPa]	[MPa]	[-]
1	2325	328,800	2	1	2264	235,500	3
2	2100	315,300	2	2	2198	271,200	2
3	1991	303,100	2	3	2335	224,800	3
4	2265	336,500	2	4	2050	291,400	2
5	2296	248,000	4	5	2013	287,500	3
6	2147	295,800	3	6	2179	-	4
Mean	2160	304,600	-	Mean	2173	262,100	-
COV	5.8%	10.4%		COV	5.7%	11.6%	

[1] In the measuring range.

3.2. Double-Sided Pullout and Calibration of Bond-Slip Law

All double-sided pullout specimens failed through pullout of all yarns. The pullout occurred randomly for each yarn at on one side or the other. For three specimen with monotonic loading, the calibration of the local bond-slip laws was performed. In Figure 3a, the calibrated functions are shown. The dashed line represents the vertical average of the three functions and was used for the following simulation of the tensile test. Note that for this specific example with relatively short embedment length compared to the full anchorage length, the direct approach to derive the local bond slip law as known from steel-reinforced concrete by division of the pullout force through the embedded length would lead to similar results as the inverse calibration.

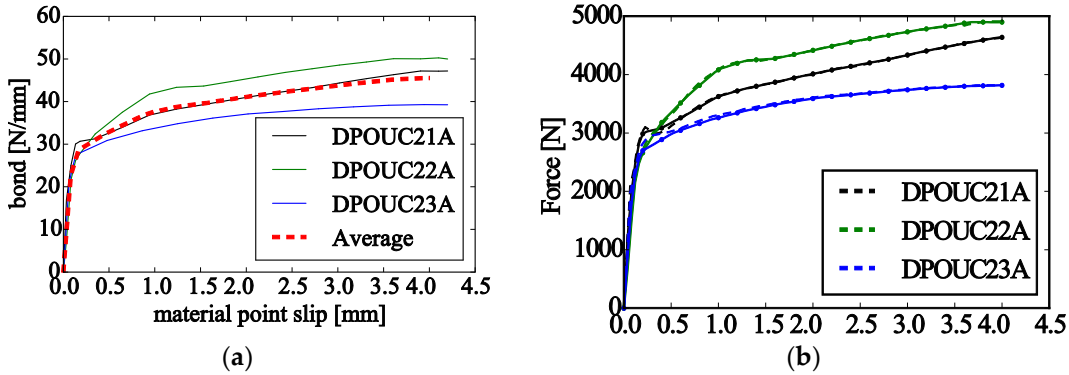

Figure 3. (**a**) Calibrated bond-slip-laws; (**b**) comparison of tests with reproduction of pullout response.

3.3. Simulation of Tensile Test with Random Matrix Strenght

To reproduce the measured stress-strain response of the uniaxial tensile specimen in the numerical simulation, the variability of the matrix strength along the test specimen must be considered in the model. Here, a Weibullian distribution of the matrix strength along the specimen length of 350 mm with an autocorrelation length of 4 mm was utilized. The scale parameter was adjusted for three different chosen values of the shape parameter with the goal to obtain the matrix stress at first cracking around the mean value of 3.2 MPa in correspondence to all 12 experiments. The random field simulation reproducing the required behavior with the desired minimum of the Weibullian random field is shown Figure 4 for the three considered values of the shape parameter.

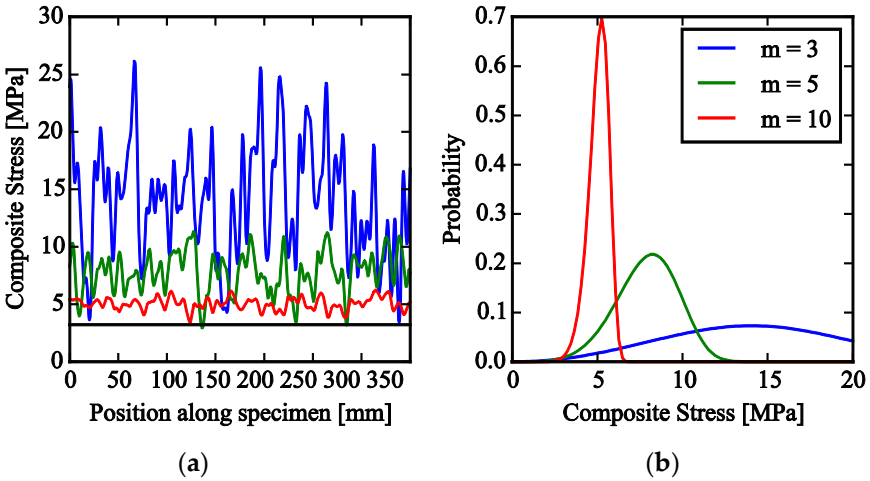

Figure 4. Simulation of tensile test (**a**) measuring range 350 mm; (**b**) measuring range 2100 mm.

In Figure 5, the results of the simulation for two different lengths are shown. Note that the number of cracks n_{cr} depends on the random position of the cracks along the specimen. Two cracks at the extremities of the specimen—as seen in the experiments near the clamping zone—enable the formation of a third crack (Figure 5a, m = 5) in a late stage of loading when sufficient stress is transmitted via bond. The longer length can be interpreted as a chain of 6 specimen, 350 mm each, with serial coupling. Thus, a comparison of the crack numbers with the experiments is possible. A high scatter of the matrix strength is reflected in a larger range of state IIa (crack formation stage).

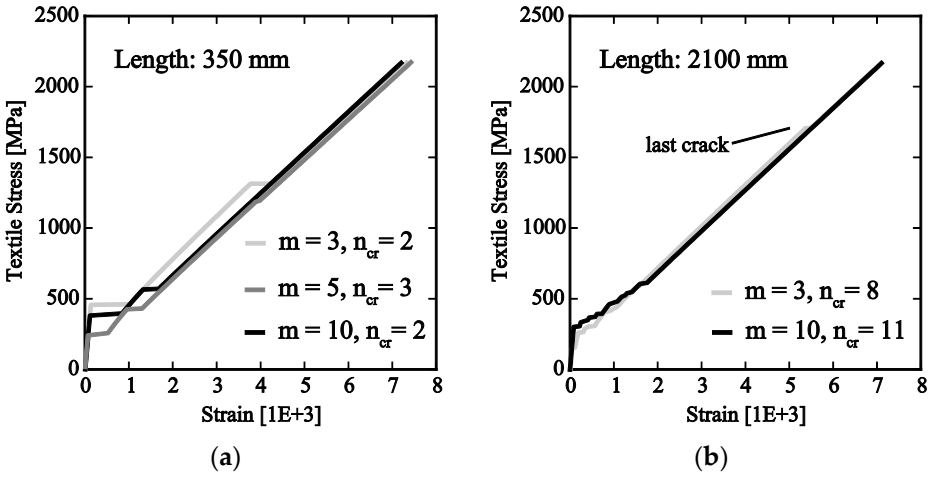

Figure 5. simulation of tensile test with random matrix strength (**a**) l = 350 mm; (**b**) l = 2100 mm.

4. Discussion and Conclusions

Unlike initially suspected, the improvement of bond characteristics in the anchorage zone for the short specimen does not influence the ultimate tensile strength of the studied fabrics significantly. This hypothesis arose from the comparison of epoxy-impregnated carbon yarns which exhibit higher tensile strength through a higher homogenization and activation of the core filaments. One explanation for this could be that the original coating with styrene-butadiene forms a sufficiently dense and closed outer layer. The secondary coating with epoxy resin is not able to penetrate through this barrier. Thus, there is no additional activation of inner filaments in the anchorage zone.

The simulation is capable of reproducing the random cracking process of the composite. The crack number and crack spacing observed in the experiments could be reproduced by utilizing the calibrated bond-slip laws. For future works, the calibration of the matrix strength random field could be obtained by utilizing a different test setup, e.g., a uniaxial tensile test of non-reinforced concrete. Thus, for a certain range of applications, it might be possible to fully replace tensile tests on the composite by a simulation based on the material characteristics of both components, matrix and reinforcement.

Author Contributions: J.B. and J.H. conceived and designed the experiments; J.B. performed the experiments; Y.L. and R.C. analyzed the data; R.C. contributed analysis tools; J.B. and R.C. wrote the paper.

Acknowledgments: This work was partly conducted in the subproject C³-V1.2 as part of the project C3—Carbon Concrete Composite, which is supported by the German Federal Ministry of Education and Research (BMBF). This support is gratefully acknowledged. The authors give their thanks to Dennis Meßerer for preparation of the specimen at HTWK Leipzig and Johannes Wendler for single-yarn tests at TU Dresden.

Conflicts of Interest: The authors declare no conflict of interest. The founding sponsors had no role in the design of the study; in the collection, analyses, or interpretation of data; in the writing of the manuscript, and in the decision to publish the results.

References

1. Bielak, J.; Hegger, J.; Chudoba, R. Towards Standardization: Testing and Design of Carbon Concrete Composites. In *High Tech Concrete: Where Technology and Engineering Meet*; Hordijk, D.A., Luković, M., Eds.; Springer International Publishing: Cham, Switzerland, 2017; pp. 313–320.
2. TUDAG. *Verfahren zur Verstärkung von Stahlbeton mit TUDALIT (Textilbewehrter Beton), 43-1.31.10-25/16*; DIBT—Deutsches Institut für Bautechnik: Berlin, Germany, 2016.
3. Schütze, E.; Bielak, J.; Scheerer, S.; Hegger, J.; Curbach, M. Uniaxial tensile test for carbon reinforced concrete with textile reinforcement. *Beton Stahlbetonbau* **2018**, *113*, 33–47.
4. Brameshuber, W.; Hinzen, M.; Dubey, A.; Peled, A.; Mobasher, B.; Bentur, A.; Aldea, C.; Silva, F.; Hegger, J.; Gries, T.; et al. Recommendation of RILEM TC 232-TDT: Test methods and design of textile reinforced concrete—Uniaxial tensile test: Test method to determine the load bearing behavior of tensile specimens made of textile reinforced concrete. *Mater. Struct.* **2016**, *49*, 4923–4927, doi:10.1617/s11527-016-0839-z.
5. Bielak, J.; Li, Y.; Hegger, J.; Chudoba, R. Numercial and Experimental Characterization of Anchorage Length for Textile Reinforced Concrete. In *Strain-Hardening Cement-Based Composites*; Mechtcherine, V., Slowik, V., Kabele, P., Eds.; Springer: Dordrecht, The Netherlands, 2017; pp. 409–417.
6. Li, Y.; Bielak, J.; Hegger, J.; Chudoba, R. An incremental inverse analysis procedure for identification of bond-slip laws in composites applied to textile reinforced concrete. *Compos. Part B Eng.* **2018**, *137*, 111–122, doi:10.1016/j.compositesb.2017.11.014.
7. Li, Y.; Chudoba, R.; Bielak, J.; Hegger, J. A modelling Framework for the Tensile Behavior of Multiple Cracking Composite. In *Strain-Hardening Cement-Based Composites*; Mechtcherine, V., Slowik, V., Kabele, P., Eds.; Springer: Dordrecht, The Netherlands, 2017; pp. 418–426.